shows the behaviour expected for the linear[6] BRAQWETS electro-optic effect

$$P_{out}(V) \propto 1 + \cos\left[\left(\frac{2\pi L}{\lambda}\right)\left(\frac{\Delta n_{WG}}{F}\right)\left(\frac{V}{w}\right) + \phi_0\right]$$

where the total thickness of undoped BRAQWETS regions $w = 0{\cdot}392\,\mu m$, ϕ_0 is the static phase difference between the two arms, and $\Delta n_{WG}/F$ is the refractive index change per applied field for the waveguide. We find an average $(\Delta n_{WG}/F) = 109 \times 10^{-12}$ m/V. This value when scaled by Γ_{8QW} indicates that the refractive index change per applied field in the quantum well layers $\Delta n_{QW}/F$ is 1500×10^{-12} m/V, about ten percent higher than expected from direct measurements of $\Delta n_{QW}/F$ in BRAQWETS.[6,†]

In the $L = 700\,\mu m$ modulator, Fig. 2 shows that 180° optical phase shift is produced by $V_\pi = 3{\cdot}2$ V single arm drive voltage. The corresponding extinction ratio (power on/power off) is 9·4 dB. For the $L = 500\,\mu m$ device, 8·9 dB extinction is obtained for $V_\pi = 5$ V. Depending on the extinction ratio required, we can choose other bias conditions. For example, in the $L = 700\,\mu m$ modulator, 8 : 1 extinction is obtained for 2·6 V and 6 : 1 for 1·8 V drive. The above modulation voltages are for single arm drive, and will be further reduced by a factor of two with both sides biased in push–pull configuration.[10] With only 1–2 V needed for large-signal modulation, high-speed voltage drivers are more readily available. In this voltage range, hybrid GaAs FET or HEMT drive electronics have been demonstrated at speeds above 20 GHz.

In conclusion, we have demonstrated Mach–Zehnder quantum well waveguide interferometers with voltage-length products one order of magnitude smaller than those that have been achieved using bulk semiconductors.‡ The sub-millimetre device lengths shown here are critical for monolithic integration of low-chirp intensity modulators with other electronic and photonic components. Drive voltages under 5 V are desirable for both monolithic and hybrid high-speed electronic drivers. Ion implantation is found to be a well-controlled, reproducible method for preparation of the ground plane and for isolation between active and passive device sections. By using this technique for electrical isolation, we can separately optimise the electrical and the optical properties of the waveguide circuit. This will be useful in future photonic circuits with larger scale of integration, where reliable, simple fabrication of electrical interconnects and electrical isolation of active sections will be of prime importance.

J. E. ZUCKER
K. L. JONES
T. Y. CHANG
N. SAUER
B. TELL
K. BROWN-GOEBELER
M. WEGENER
D. S. CHEMLA

AT&T Bell Laboratories, Holmdel, New Jersey 07733, USA

19th September 1990

† Given the refractive index change per applied field $\Delta n/F$ at one wavelength, $\Delta n/F$ at another wavelength can be estimated because the BRAQWETS $\Delta n/F$ falls off as $1/\Delta\omega$, where $\Delta\omega$ is the energy difference between the below-gap operating wavelength and the ground-state exciton peak wavelength; thus $(\Delta n/F)]_{\Delta\omega_2} \sim (\Delta n/F)]_{\Delta\omega_1} \times (\Delta\omega_1/\Delta\omega_2)$

‡ A. Gnauck (unpublished)

References

1 OKIYAMA, T., NISHIMOTO, H., YOKOTA, I., and TOUGE, T.: 'Evaluation of 4-Gbit/s optical fiber transmission distance with direct and external modulation', *J. Lightwave Technol.*, 1988, **6**, p. 1686

2 HALEMANE, T. R., and KOROTKY, S. K.: 'Distortion characteristics of optical directional coupler modulators', *IEEE Trans.*, 1990, **MTT-38**, p. 669

3 SUZUKI, M., NODA, Y., TANAKA, H., AKIBA, S., KUSHIRO, Y., and ISSHIKI, H.: 'Monolithic integration of InGaAsP/InP distributed feedback laser and electroabsorption modulator by vapor phase epitaxy', *J. Lightwave Technol.*, 1987, **5**, p. 1277

4 SODA, H., FURUTSU, M., SATO, K., OKAZAKI, N., YAMAZAKI, Y., NISHIMOTO, H., and ISHIKAWA, H.: 'High-power and high-speed semi-insulating BH structure monolithic electroabsorption modulator/DFB laser light source', *Electron. Lett.*, 1990, **26**, (1), pp. 9–10

5 KOYAMA, F., and IGA, K.: 'Frequency chirping in some types of external modulators', *J. Lightwave Technol.*, 1988, **6**, p. 87

6 ZUCKER, J. E., CHANG, T. Y., WEGENER, M., SAUER, N. J., JONES, K. L., and CHEMLA, D. S.: 'Large refractive index changes in tunable-electron-density InGaAs/InAlAs quantum wells', *IEEE Photonics Technol. Lett.*, 1990, **2**, p. 29

7 WEGENER, M., ZUCKER, J. E., CHANG, T. Y., SAUER, N. J., JONES, K. L., and CHEMLA, D. S.: 'Absorption and refraction spectroscopy of a tunable-electron-density quantum-well and reservoir structure', *Phys. Rev. B.*, 1990, **41**, p. 3097

8 ZUCKER, J. E., JONES, K. L., MILLER, B. I., and KOREN, U.: 'Miniature Mach–Zehnder InGaAsP quantum well waveguide interferometers for 1·3 μm', *IEEE Photon. Technol. Lett.*, 1990, **2**, p. 32

9 ZUCKER, J. E., WEGENER, M., JONES, K. L., CHANG, T. Y., SAUER, N., and CHEMLA, D. S.: 'Optical waveguide intensity modulators based on a tunable electron density multiple quantum well structure', *Appl. Phys. Lett.*, 1990, **56**, p. 1951

10 TAKEUCHI, H., KASAYA, K., and OE, K.: 'Low-switching-voltage InGaAsP/InP waveguide interferometric modulator for integrated optics', *IEEE Photon. Technol. Lett.*, 1990, **1**, p. 227

APPROXIMATE EXPRESSION FOR NORMALISED THROUGHPUT OF MULTISTAGE INTERCONNECTION NETWORKS

Indexing terms: Telecommunication, Networks, Switching

An alternative formula is presented for the normalised throughput of unbuffered multistage interconnection networks (MINs). From the alternative formula, an approximate expression is derived. Numerical results show that the approximate expression can provide excellent estimates of the normalised throughputs. Moreover, the asymptotic performance of MINs can be determined as well.

Introduction: The normalised throughput, which is defined as the average number of packets received by an outlet per network cycle, is often adopted as the performance measure of unbuffered multistage interconnection networks (MINs) in a packet switched environment. Under the uniform traffic model, the normalised throughput of an MIN can be evaluated iteratively[1] or recursively.[2] The normalised throughput basically is a function of the input rate, the number of stages, and the size of switching elements. However, the iterative or recursive procedure mentioned above has to be performed again if the input rate is changed. Furthermore, the asymptotic behaviour of MINs can not be easily determined by those procedures.

In this letter, we will present an alternative formula for the normalised throughput of MINs composed of α-input and β-output switching elements. From this formula, we then derive an approximate expression which can provide excellent estimates of the normalised throughputs as well as the asymptotic performance of MINs. When $\alpha = \beta$ (i.e. square MINs), our approximate expression agrees with the one derived by Kruskal and Snir.[3]

Alternative formula: Consider an n-stage MIN composed of α-input and β-output switching elements. For convenience, the α^n inlets and β^n outlets are numbered from top to bottom by 0 to $\alpha^n - 1$ and 0 to $\beta^n - 1$, respectively. As usual, the normalised throughput is chosen as the performance measure in our study. The following assumptions are necessary to us when the normalised throughput is analysed.

(1) Packets are generated at inlets independently with identical rates denoted by ρ.

(2) Each packet is assumed to be destined to any outlet equally likely.

(3) A switching element will randomly select a packet with equal probability and reject the others when a conflict occurs. Because the traffic is uniform, it is sufficient to consider the average throughput of a particular outlet, say outlet 0.

In the n-stage network, let $w_n(c_1, c_2, \ldots, c_m)$ denote the number of distinct links inside switching elements traversed by the paths connecting different inlets $c_1, c_2, \ldots$ and $c_m (c_1 < c_2 < \cdots < c_m)$, to outlet 0. For example, $w_2(0, 1) = w_2(0, 2) = w_2(0, \alpha - 1) = 3$ (see the broken lines in Fig. 1).

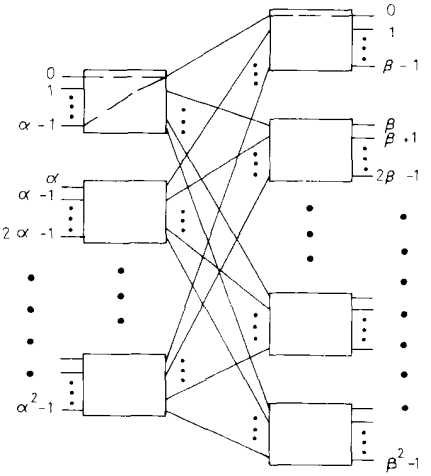

Fig. 1 *Illustration of* $w_2(0, \alpha - 1) = 3$

Let S_n and ρ denote, respectively, the normalised throughput and the input rate of the investigated MIN. Then we have

$$S_n = \sum_{m=1}^{\alpha^n} (-1)^{m-1} r_m \tag{1}$$

where

$$r_m = \rho^m \sum_{c_1=1}^{\alpha^n - m} \sum_{c_2=c_1+1}^{\alpha^n - m + 1} \cdots \sum_{c_m=c_{m-1}+1}^{\alpha^n - 1} \left(\frac{1}{\beta}\right)^{w_n(c_1, c_2, \ldots, c_m)}$$

Eqn. 1 can be proved by mathematical induction. However, owing to space limitations, the proof is omitted.

Approximate expression: In reality, S_n can be expressed as a polynomial of the input rate ρ. That is,

$$S_n = a_1\rho - a_2\rho^2 + \ldots - a_{\alpha^n}\rho^{\alpha^n} \tag{2}$$

where

$$a_m = \sum_{c_1=1}^{\alpha^n - m} \sum_{c_2=c_1+1}^{\alpha^n - m + 1} \cdots \sum_{c_m=c_{m-1}+1}^{\alpha^n - 1} \left(\frac{1}{\beta}\right)^{w_n(c_1, c_2, \ldots, c_m)}.$$

To determine the coefficients that appear in eqn. 2, a tree diagram is used here. It is not hard to see that the paths from all the inlets to a particular outlet form a tree of $m + 1$ levels. The outlet is represented by the root located at level 0. Inlets are represented by vertices located at level n and are labelled by integers 0 to $\alpha^n - 1$ so that vertex i corresponds to inlet i. Each edge in this tree corresponds to a link inside a switching element of the original network. A vertex is said to be a descendant of another vertex if it is a child of that vertex or a child of some descendant of that vertex. To determine the value of a_m, a count has to be made of the total number of edges in those paths connecting i distinct vertices located at level n to the root. Every edge traversed by at least one of those paths is counted exactly once even if it is shared by several paths. As an example, as the distance from each vertex at level n to the root is always equal to n, we have $w_n(c_i) = n$ for any i. Therefore, a_1 is given by

$$a_1 = \sum_{i=1}^{\alpha^n} (1/\beta)^n = (\alpha/\beta)^n$$

To compute the value of a_2, we consider the vertices located at level $n - 1$ first. Each considered vertex has α descendants. If we select any two vertices c_1 and c_2 from the α vertices, then $w_n(c_1, c_2) = n + 1$. As there are α^{n-1} vertices located at level $n - 1$, we know that the number of (c_1, c_2) pairs which result in $w_n(c_1, c_2) = n + 1$ is equal to $\binom{\alpha^{n-1}}{1}\binom{\alpha}{2}$. Next, consider the vertices located at level $n - 2$. For each considered vertex, there are α^2 descendants located at level n. These α^2 descendants can be partitioned into α groups so that all the vertices in the same group have the same father. If we choose any two vertices c_1 and c_2 from different groups, then we have $w_n(c_1, c_2) = n + 2$. The cases where both vertices are selected from the same group had been considered when vertices at level $n - 1$ were inspected. Thus, the total number of vertex pairs (c_1, c_2) which yield $w_n(c_1, c_2) = n + 2$ is equal to $\binom{\alpha^{n-2}}{1}\binom{\alpha}{2}\binom{\alpha}{1}\binom{\alpha}{1}$. Similarly, one can verify that the number of vertex pairs (c_1, c_2) which yield $w_n(c_1, c_2) = n + i$ is $\binom{\alpha^{n-i}}{1}\binom{\alpha}{2}\binom{\alpha^{i-1}}{1}\binom{\alpha^{i-1}}{1}$. Consequently, a_2 is given by

$$a_2 = \sum_{i=1}^{n} \alpha^{n-i}\binom{\alpha}{2}\binom{\alpha^{i-1}}{1}\binom{\alpha^{i-1}}{1}(1/\beta)^{n+i}$$

The values of $a_3, a_4, \ldots$ and a_{α^n} can be similarly derived. If the number of stages n is sufficiently large, then a_i can be approximated by

$$a_i \approx (\alpha/\beta)^n \left[\frac{(\alpha - 1)}{2\beta} \frac{1 - (\alpha/\beta)^n}{1 - (\alpha/\beta)}\right]^{i-1}$$

After substituting the approximation of a_i into eqn. 2, we get

$$S_n \approx (\alpha/\beta)^n \frac{\rho}{1 + \dfrac{(\alpha - 1)}{2\beta} \dfrac{1 - (\alpha/\beta)^n}{1 - (\alpha/\beta)} \rho} \tag{3}$$

For the special case when $\alpha = \beta$, eqn. 3 becomes

$$S_n \approx \frac{\rho}{1 + \dfrac{(\alpha - 1)n}{2\alpha}} \tag{4}$$

which was also obtained by Kruskal and Snir[3] using a different approach.

Results and discussion: Notice that eqn. 3, which can be used to compute the approximate normalised throughput, represents the asymptotic performance of MINs. As the switching elements are not square, the average number of packets successfully transmitted by each inlet per network cycle is equal to $(\beta/\alpha)^n S_n$. Moreover, one can verify that, for large values of n, S_n/S_{n-1} is roughly equal to α/β if $\alpha/\beta < 1$ or 1 if $\alpha/\beta \geq 1$.

Fig. 2 shows the comparison between the normalised throughput computed by eqn. 3 and the exact values against input rate ρ for $\alpha = 2$ and $\beta = 4$. The approximation is consistently larger than the exact value for any values of ρ and n. However, the relative error, i.e. the ratio of the difference

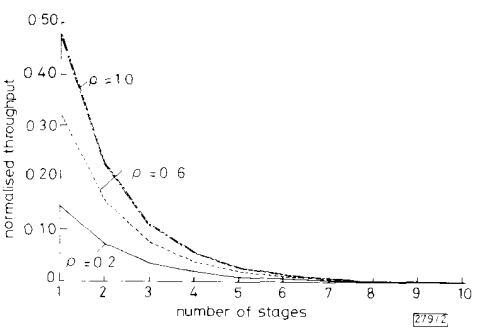

Fig. 2 *Normalised throughput against number of stages for* $\alpha = 2, \beta = 4$
—·—·— exact value
—·—·— approximation

between approximation and exact value to the exact value, is within 2%. Fig. 3 shows similar results for square MINs. The

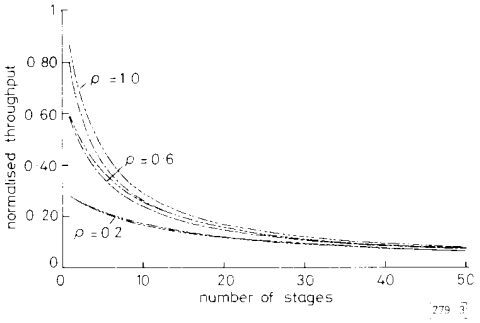

Fig. 3 *Normalised throughput against number of stages for* $\alpha = \beta = 2$
—·—· exact value
—— approximation

relative error is within 5·5% providing $n > 20$. Numerical results reveal that our approximate expression can quickly provide excellent estimates of the normalised throughputs for large MINs at any traffic load.

T.-H. LEE
J.-J. CHOU

Department of Communication Engineering
Institute of Electronics
National Chiao Tung University
Hsinchu, Taiwan 30050
Republic of China

28th September 1990

References

1 PATEL, J. H.: 'Performance of processor-memory interconnections for multiprocessors', *IEEE Trans.*, October 1981, **C-30**, pp. 771–780
2 LEE, T. H.: 'Performance of banyan networks with inhomogeneous traffic flow', *IEE Proc. E*, 1990, **137**, (4), pp. 245–252
3 KRUSKAL, C. P., and SNIR, M.: 'The performance of multistage interconnection network', *IEEE Trans.*, 1983, **C-32**, (12), pp. 1091–1098
4 GOKE, L. R., and LIPOVSKI, G. J.: 'Banyan network for partitioning multiprocessor system'. Proc. of first Ann. Symp. on Comp. Arch. 1973, pp. 21–30

WAVELENGTH-TUNABLE SINGLE-FREQUENCY AND SINGLE-POLARISATION Er-DOPED FIBRE RING-LASER WITH 1·4 kHz LINEWIDTH

Indexing term: Lasers

A narrow linewidth of 1·4 kHz with single frequency operation is demonstrated in an Er-doped fibre ring-laser. A stable lasing spectrum can be achieved using a single-polarisation fibre-cavity. An optical bandpass filter incorporated in the ring-cavity makes the lasing wavelength tunable, and a 2·8 nm tuning range is demonstrated.

Narrow linewidth, single-frequency laser sources are attractive for optical coherent communications and optical fibre sensors, especially in homodyne detection systems.*,‡,[1] Much effort has been made to narrow the linewidths of Er-doped or Nd-doped fibre-lasers by using fibre gratings in the Fabry–Perot fibre-cavity[2–4] or fibre Fox–Smith resonators.[5] However, the obtained linewidths to date are more than 1 MHz. Recently, an Er-doped single-mode-fibre ring-laser with a 60 kHz linewidth has been demonstrated by introducing unidirectional operation, thus eliminating the spatial hole burning.[6] We constructed a unidirectional Er-doped fibre ring-laser with all polarisation-holding fibres and inserted a narrow optical bandpass filter to achieve the lasing wavelength tunability and stable lasing spectrum without polarisation-mode competition. A linewidth of 1·4 kHz was measured with single frequency operation.

Fig. 1 shows the experimental configuration of the Er-doped single-polarisation fibre-ring laser including the linewidth measurement setup. A 1·48 μm CW Fabry–Perot

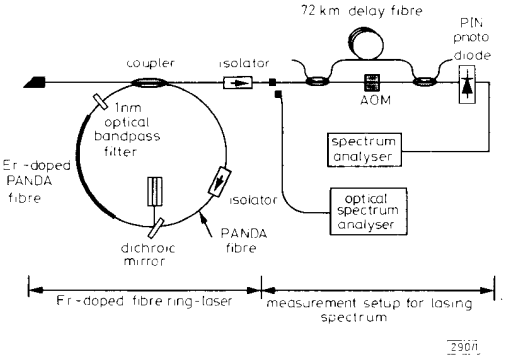

Fig. 1 *Experimental setup of Er-doped fibre-ring-laser including delayed self-heterodyne interferometer*

laser diode was used as the pump source. The pump beam was coupled into the cavity through a dichroic mirror. The dichroic mirror has a high reflectivity ($R \simeq 100\%$) at the pumping wavelength and high transmission ($T = 95\%$) at the lasing wavelength. A 15 m Er-doped polarisation-holding fibre with an SiO_2 core was used as the laser medium. The Er-dopant concentration was 300 ppm. A polarisation-holding fibre-coupler was employed to take out 10% of the lasing power from the cavity. The unidirectional operation was achieved by inserting a polarisation-holding fibre-pigtailed isolator with a 60 dB isolation ratio into the ring-cavity. The extinction ratio between the two orthogonal polarisation states of the isolator was 25 dB. Single-polarisation operation was achieved through the prevention of two polarisation-mode competition.[7] The free spectrum range (FSR) of the ring-cavity was 9·2 MHz. An optical bandpass filter with a 1 nm bandwidth was also inserted in the ring-cavity for wavelength tunability. The unwanted reflections were prevented by terminating the fibre-ends and introducing an isolator. The fibre components were incorporated into the ring-cavity by fusion splicing.

Fig. 2 shows the output laser power as a function of the pump power. The threshold occurred at 50 mW and a

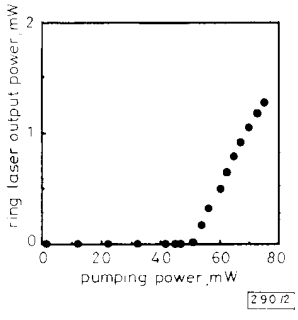

Fig. 2 *Output laser power as function of laser diode pumping power*

* IWATSUKI, K., OKAMURA, H., and SARUWATARI, M.: 'Optical homodyne detection with a injection-locked Er-doped-fibre-ring-laser'. Submitted to *Opt. Lett.*
‡ OKAMURA, H., and IWATSUKI, K.: 'Fibre-optic sensor using an injection-locked local laser'. Submitted to 7th Optical Fibre Sensors Conference